PHYSICAL REVIEW B VOLUME 33, NUMBER 11 1 JUNE 1986

Evidence for locally correlated spin canting in the reentrant spin-glass state of Au-Fe alloys

M. M. Abd-Elmeguid and H. Micklitz
Institut für Experimentalphysik IV, Ruhr Universität Bochum, D-4630 Bochum, Federal Republic of Germany

R. A. Brand and W. Keune
Laboratorium für Angewandte Physik, Universität Duisburg, D-4100 Duisburg, Federal Republic of Germany
(Received 22 November 1985; revised manuscript received 7 March 1986)

We report what we believe to be the first ^{197}Au Mössbauer experiments on Au-Fe alloys in the spin-glass and reentrant region (8, 15.7, and 16.8 at.% Fe) in the temperature range 77–4.2 K. The temperature dependence of the mean value $\bar{B}_{\rm thf}$ of the transferred magnetic hyperfine field at the ^{197}Au site in the 16.8-at.%-Fe sample shows the spin-canting transition at $\tilde{T}_f$. Analysis of $\bar{B}_{\rm thf}(T)$ gives evidence that this spin canting is not random, but is locally correlated.

The interpretation of the magnetic double transition observed in Au-Fe alloys near the percolation threshold by means of ^{57}Fe Mössbauer spectroscopy[1,2] has been questioned recently.[3] The reentrant transition from the ferromagnetic (FM) state to the spin-glass- (SG) like state at the temperature $\tilde{T}_f$ has been explained[1,2,4,5] on the basis of the so-called spin canting predicted by Gabay and Toulouse (GT)[6] in the infinite-range model with Heisenberg spins. Quite in contrast to this interpretation, a simple "two-phase" model was proposed by Violet and Borg[3] to explain the transition at $\tilde{T}_f$. In order to add more experimental data to this controversial subject, and to gain more insight into the nature of this spin canting, we have performed ^{197}Au Mössbauer-effect (ME) experiments on Au-Fe samples near and above the percolation threshold. This is to our knowledge the first time that such experiments have been performed. Previous ^{197}Au ME experiments reported by Borg and Pipkorn[7] were limited to the spin-glass region (their maximum concentration of 15 at.% Fe was too low to observe the reentrant transition[8]). The advantage of the ^{197}Au compared to the commonly used ^{57}Fe ME resonance is the following: The Au atoms do not carry any magnetic moment. The magnetic hyperfine (hf) field measured at the ^{197}Au site in Au-Fe alloys, called the transferred hyperfine field $B_{\rm thf}$, thus reflects the local distribution of the Fe moments (atoms) as well as the local correlation of the Fe-moment directions. This means that we can probe not only the chemical homogeneity but also the local spin texture and its change with temperature T by measuring $\bar{B}_{\rm thf}(T)$.

The main results of our experiments are as follows: (i) The hf distribution $P(B_{\rm thf})$ can be reasonably approximated by a binomial distribution using the *nominal* Fe atomic concentration. This shows that the Fe atoms are rather homogeneously distributed in the Au-Fe alloy. (ii) The temperature dependence of the average value $\bar{B}_{\rm thf}$ shows the same canting transition at $\tilde{T}_f$, exactly as the average effective field $B_{\rm eff}$ at the ^{57}Fe site[1,2] does. The latter point has an important consequence for the nature of the spin-canting transition in the Au-Fe alloys. The variation of $\bar{B}_{\rm thf}(T)$ at the ^{197}Au site gives direct evidence that *the spin canting of the Fe moments is correlated on a local scale below* $\tilde{T}_f$.

^{197}Au ME experiments are reported on here from two different Au-Fe samples (see inset in Fig. 1 for details). Sample 1 with 8 at.% Fe is well below the critical concentration for reentrant behavior. Sample 2 with 16.8 at.% Fe, which is the *same* sample as that used in Ref. 1, shows reentrant behavior. Both samples were foils of $\simeq 6\ \mu$m thickness, solution annealed at about 900 °C in vacuum for 49 h, and rapidly quenched in water. The ^{197}Pt ME source was obtained by neutron irradiation (flux 1.4×10^{14} $n/{\rm cm}^2{\rm s}^1$) of an enriched Pt foil ($\simeq 98\%$ ^{196}Pt) of $\simeq 20\ \mu$m thickness for 2 days, resulting in a source activity of $\simeq 40$ mCi. An intrinsic Ge detector was used for counting the 77.3-keV γ quanta. Count rates up to 10^5 counts/s in the single-channel window could be handled with our detection system. ME spectra were taken with absorber temperatures between 4.2–77 K, while the source was always at 4.2 K.

Figure 1 shows representative ^{197}Au ME spectra corresponding to the four points, 1A and 1B for sample 1, and 2A and 2B for sample 2, shown in the phase diagram in the inset. Point 1A is in the paramagnetic (PM) state ($T=77$ K) and 1B is in the SG state ($T=4.2$ K). For sample 2, 2A is in the reentrant FM ($T=55$ K), and 2B is in the reentrant SG (like) state ($T=4.2$ K). The curves through the data points are least-squares fits using the histogram model (see below).

Let us first discuss spectrum 1A (8 at.% Fe at $T=77$ K), in the PM state, which is rather symmetric. This has been fitted using an isomer-shift distribution with the binomial model (see below). We have also obtained and fitted a similar symmetric spectrum for an Au–15.8 at.%-Fe sample at 55 K, close to the Curie temperature T_c. From these facts we can conclude that the quadrupole interaction can be neglected in the further analysis of the ^{197}Au ME spectra. This is in contrast to the analysis proposed by Borg and Pipkorn[7] who assumed, in addition, significant quadrupole interaction at the ^{197}Au site. This point will be discussed later. The strong asymmetry observed in the magnetically ordered state (both 1B and 2B in Fig. 1) is thus *not* caused by the quadrupole interaction, but is due to *a strong correlation between the ME isomer shift S and* B_{thf}. We assume for simplicity a linear correlation between S and $B_{\rm thf}$, i.e., $S=S_0+\alpha B_{\rm thf}$. S_0 is the isomer shift of ^{197}Au in pure Au relative to the ^{197}Au:*Pt* ME source [$S_0=-1.2$ mm/s (Ref. 9)]. The order of magnitude of α can be estimated from the known isomer-shift difference ΔS between ^{197}Au in Fe and that in Au [$\Delta S=+5.4$ mm/s (Ref. 9)] and the observed $B_{\rm thf}$ for dilute ^{197}Au in Fe [$B_{\rm thf}=-128$ T (Ref. 10)] to be

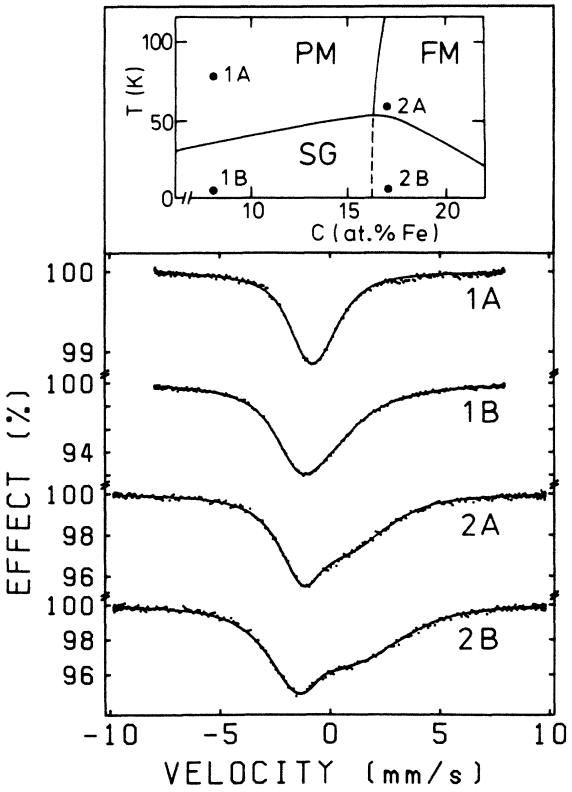

FIG. 1. ^{197}Au ME spectra of Au: 8 at.% Fe, and Au: 16.8 at.% Fe at selected temperatures. The inset shows the magnetic phase diagram of Au-Fe alloys (Ref. 8) (PM paramagnetic, FM ferromagnetic, and SG spin-glass states). The four spectra correspond to the points given in this diagram as 1A and 1B for 8 at.%, and 2A and 2B for 16.8 at.% Fe.

$\alpha = \Delta S/|B_{\rm thf}| \simeq +0.04$ mms^{-1}T^{-1}. Using a linear correlation with α as a free-fitting parameter, we have analyzed the ^{197}Au ME spectra with two different models in order to obtain a model-independent hf distribution $P(B_{\rm thf})$.

The first model uses a histogram method and does not make any assumptions on the shape of $P(B_{\rm thf})$. The distribution $P(B_{\rm thf})$ is just given by a histogram ranging (in our case) from $B_{\rm thf}=0$ to $B_{\rm thf}|_{\rm max}$ with i steps ($i=0$ to $i_{\rm max}$) and constant step width ΔB, i.e., is given by the set: $P(B_{\rm thf}) = P_i(B_i)$, with $B_i = i\Delta B$, and $i=0,1,\ldots,i_{\rm max}$. The step width was set $\Delta B = 5$ T and number of steps $i_{\rm max} \simeq 20$, corresponding to $B_{\rm thf}|_{\rm max} \simeq 100$ T.

In contrast to the first model, we have assumed, as well, a second binomial (histogram) model, where the shape of $P(B_{\rm thf})$ is given by a binomial distribution of variable step width, i.e., is given by the set $P(B_{\rm thf}) = P_n(B_n)$, with

$$P_n = \binom{12}{n}(1-c)^{12-n}c^n ,$$

where $B_n = nB_0$ and $n=0,1,\ldots,12$. c is the *nominal* Fe atomic concentration, n the number of nearest-neighbor NN Fe atoms for the Au site in the fcc Au matrix (12 NN atoms), and B_0 is the only free-fitting parameter describing $P(B_{\rm thf})$ in this model. Several assumptions enter this model: (i) the alloy is homogeneous; (ii) $B_{\rm thf}$ is given essentially by the Fe NN contributions (those from non-NN Ruderman-Kittel-Kasuya-Yosida) interactions etc., are neglected); and (iii) these NN contributions can be treated as additive, i.e., the few Fe NN atomic moments are parallel among themselves (there are on the average about 2 NN Fe atoms at 16.8 at.% Fe).

Figure 2 shows the distribution $P(B_{\rm thf})$ of sample 2 (16.8 at.% Fe) at $T=55$ and 4.2 K as obtained from these two models. The free-fitting parameters from the binomial model are found to be $\alpha \simeq +0.04$ and $+0.03$ mms^{-1}T^{-1}, and $B_0 = 13.2$ and 18.6 T, at 55 and 4.2 K, respectively. α is in rather good agreement with the value estimated above. B_0 at 4.2 K is of the same order of magnitude as B_0 for ^{197}Au found in bcc Fe [$B_{\rm thf} = 8B_0 \simeq 128$ T (Ref. 10)]. The agreement in $P(B_{\rm thf})$ between the two different distribution models is striking. This shows clearly that the assumptions which enter into the binomial model are justified. From this we conclude that *the Fe atoms are rather homogeneously distributed in our samples.* Our results do not exclude the existence of some atomic short-range order in the sample; however, the analysis of the data clearly shows a continuous distribution over many sites (see Fig. 2). This strongly contrasts the conclusions derived by Violet and Borg[3] for the existence of two different "phases" with strongly different Fe concentrations which would cause a broad asymmetrical line shape at the ^{197}Au site in the PM state as well,[7] which we do not observe in our samples. We feel that the differences in conclusions between the present work and Refs. 3 and 7 are mainly related to differences in sample preparation.

Our findings on the state of our samples are, on the other hand, essentially in agreement with those of Whittel and Campbell.[11] They concluded from a careful analysis of the quadrupole splitting in the room-temperature ^{57}Fe ME spectra of the Au-Fe alloys that the Warren-Cowley chemical short-range-order parameter $\sigma_{\rm WC} = (c'-c)/(1-c)$ (where c is the nominal, and c' the concentration, in the NN shell) is rather small and dependent on sample heat treatment.

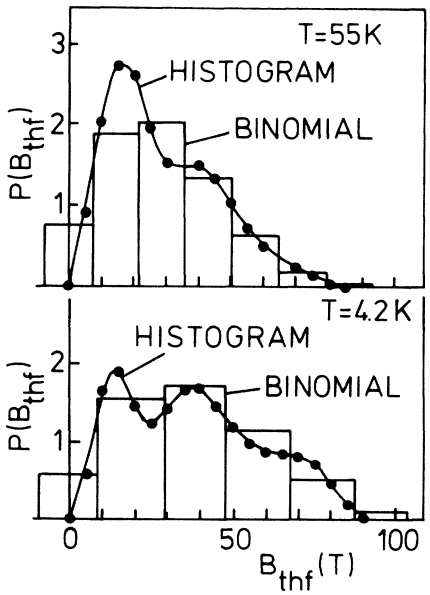

FIG. 2. Distribution of the transferred hyperfine magnetic field $B_{\rm thf}$ at the ^{197}Au site in Au: 16.8 at.% Fe at $T=55$ and 4.2 K. The two different distributions for each temperature correspond to the histogram and the binomial model as described in the text.

They find $\sigma_{WC} \simeq -0.04$ for a quenched, and $+0.05$ for a cold-worked Au–15-at.%-Fe alloy. Note that the quenched alloy shows slight *anti*clustering.

In the next step, the temperature dependence of the average $\bar{B}_{thf}$ was carefully analyzed for the reentrant sample 2 (16.8 at.% Fe) in the range from 4.2–55 K using the binomial model. The average field as given by $\bar{B}_{thf} = \sum B_n P(B_n)$ is shown in Fig. 3, together with the average $\bar{B}_{eff}$ previously measured at the ^{57}Fe site of the *same* sample.[1] The most interesting feature of $\bar{B}_{thf}(T)$ is the break in slope at the temperature $\tilde{T}_f$ which appears in the $\bar{B}_{eff}(T)$ results at the ^{57}Fe site as well. This increase in $\bar{B}_{eff}(^{57}\text{Fe})$ below $\tilde{T}_f$, observed by Lauer and Keune,[1] and Varret, Hamzić, and Campbell[2] as well, has been interpreted as being due to the freezing of the transverse component S_t of the local Fe moment S, which occurs at the transition to the reentrant spin-glass state[2,4,5] (see inset to Fig. 3; S, S_z, and S_t denote thermal expectation values, and z is the direction of the spontaneous magnetization in the FM state). In the FM state, B_{eff} measured S_z only, due to spin precession. The nonzero value of S_t for $T < T_f$, together with S_z, yields a larger effective S, and thus B_{eff} (^{57}Fe), in the reentrant SG state. The meaning of the results presented in Fig. 3 is that we measure about the same change in the hyperfine field $\bar{B}_{thf}$ at the ^{197}Au site as well. The local field at the ^{197}Au site induced from one Fe NN will be denoted as h. The components h_z and h_t are defined in a similar fashion to those of the Fe moment shown in the inset to Fig. 3, S_z and S_t. The value extrapolated to $T = 0$ K from $\bar{B}_{thf}(T)$ from data for $T < T_f$, $\bar{B}_{thf}(0;\text{SG})$, is $\simeq 26\%$ larger than that extrapolated from $T > T_f$, $\bar{B}_{thf}(0;\text{FM})$. The ratio

$$R(^{197}\text{Au}) \equiv \bar{B}_{thf}(0;\text{SG})/\bar{B}_{thf}(0;\text{FM}) = 1.26$$

is only slightly smaller than that found for the ^{57}Fe site, $R(^{57}\text{Fe}) = 1.30$. Now we want to show how this observation gives us information about the spin structure in the reentrant canted SG state. B_{thf} (^{197}Au) at a given site results from the contributions of *all* the NN Fe atoms. The ratio R defined above is thus for one Au site

$$\left[1 + \left(\sum_i h_{t,i} \Big/ \sum_i h_{z,i}\right)^2\right]^{1/2} ,$$

where the sum over i extends over the n Fe NN moments for a given configuration. Assuming all local contributions to be equal, we can write, averaging over all Au sites

$$R \simeq [1 + (h_t/h_z)^2 \langle n^{-1} \rangle]^{1/2} ,$$

where n is the number of Fe NN's and angle brackets indicate averaging over all possible configurations $n > 0$. In the case of complete correlation at every site, $\langle n^{-1} \rangle$ is replaced by 1, so that $R_{corr} = R(^{57}\text{Fe}) = 1.30$ (assuming only that $|h_t/h_z| = |S_t/S_z|$). For the random case, we have calculated the above average over the binomial distribution, and obtain, for 16.8 at.% Fe, a result of $R_{ran} = 1.12$ [estimating $(h_t/h_z)^2$ from $R(^{57}\text{Fe})$]. These two limits are shown in Fig. 3 as well. The fact that our observed value of $R \simeq 1.26$ is much closer to R_{corr} than it is to R_{ran} (see Fig. 3) shows that in the reentrant SG state, the moments of the NN Fe atoms are canted in nearly the same direction. Thus, our

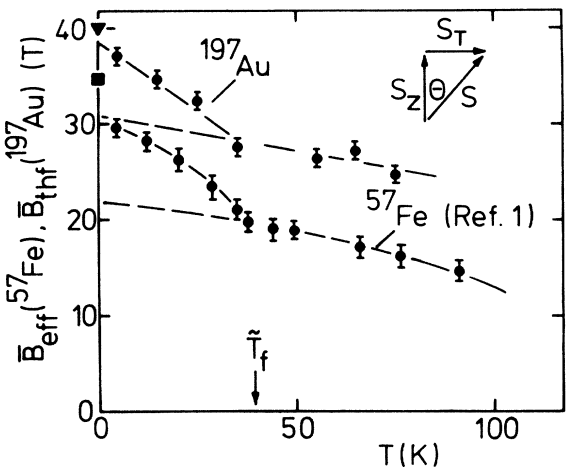

FIG. 3. Temperature dependence of the average value $\bar{B}_{thf}$ in ^{197}Au: 16.8 at.% Fe. $\tilde{T}_f$ gives the temperature of the transition into the reentrant SG state. Also shown is the temperature dependence of the $\bar{B}_{thf}$ found at ^{57}Fe site in the *same* sample (from Ref. 1). The square and triangular points give the extrapolated $\bar{B}_{thf}(0;\text{SG})$ as calculated from R_{ran} and R_{corr}, respectively. The lines through the data are a guide to the eye only. The inset shows the components of the Fe moment S, S_z, and S_t (the ^{197}Au hf field components are h, h_z, and h_t, in a similar manner).

^{197}Au ME results give unequivocal evidence that the *spin canting in Au-Fe reentrant alloys is correlated on a local scale.* (It is certain that the correlation is not macroscopic, since in that case the ^{57}Fe ME results *in external magnetic field* would have been different than those presented in Refs. 1 and 2.)

We should mention here several other non-ME experiments in which the magnetic double transition in Au-Fe alloys has been studied. Neutron scattering experiments by Murani[12] show an increase of magnetic correlation below $\tilde{T}_f$. This increase, however, was not discussed in terms of spin canting (the GT model appeared one year later), but rather was attributed to an increase in the FM correlation length due to long-ranged RKKY interactions which were supposed to become more important below $\tilde{T}_f$. Perturbed angular correlation experiments on ^{111}Cd as a probe in Au-Fe alloys[13] also showed an increase in the transferred hf field at the ^{111}Cd impurity site starting well below the Curie temperature. These authors, however, were hesitant about drawing any conclusions about the Fe spin structure below $\tilde{T}_f$ from this observation.

We note that these new results help to confirm the canting model of the transition at $\tilde{T}_f$, and add important new insight unavailable from previous studies. Evidence is found that the Fe atomic distribution is reasonably homogeneous in these quenched alloys, and that the spin canting observed occurs in a locally correlated manner. This clarifies the explanation proposed by Brand, Lauer, and Keune[5] for the ^{57}Fe quadrupole line shift observed below $\tilde{T}_f$.

This work was supported by the Deutsche Forschungsgemeinschaft (Sonderforschungsbereich No. 166 Duisburg-Bochum).

[1]J. Lauer and W. Keune, Phys. Rev. Lett. **48**, 1850 (1982).

[2]F. Varret, A. Hamzić, and I. A. Campbell, Phys. Rev. B **26**, 5195 (1982).

[3]C. E. Violet and R. J. Borg, Phys. Rev. Lett. **51**, 1073 (1983); in *Proceedings of the ICAME 1985, Leuven* [Hyperfine Interact. (to be published)]; R. J. Borg and T. A. Kitchens, J. Phys. Chem. Solids **34**, 1323 (1973). See references to the similar platelet model of P. Beck in Ref. 5.

[4]R. A. Brand, V. Manns, and W. Keune, in *Heidelberg Colloquium on Spin Glasses,* edited by J. L. vanHemmen and I. Morgenstern, Lecture Notes in Physics, Vol. 192 (Springer, Heidelberg, 1983).

[5]R. A. Brand, J. Lauer, and W. Keune, Phys. Rev. B **31**, 1630 (1985).

[6]M. Gabay and G. Toulouse, Phys. Rev. Lett. **47**, 201 (1981).

[7]R. J. Borg and D. N. Pipkorn, J. Appl. Phys. **40**, 1483 (1969).

[8]G. J. Nieuwenhuys, B. H. Verbeek, and J. H. Mydosh, J. Appl. Phys. **50**, 1685 (1979).

[9]P. H. Barrett, R. W. Grant, M. Kaplan, D. A. Keller, and D. A. Shirley, J. Chem. Phys. **39**, 1035 (1963).

[10]B. N. Samoilov, V. V. Sklyareskii, and V. D. Gorobchenko, Zh. Eksp. Teor. Fiz. **41**, 1783 (1961) [Sov. Phys. JETP **14**, 1267 (1962)].

[11]G. L. Whittel and S. J. Campbell, J. Phys. F **15**, 693 (1985).

[12]A. P. Murani, Solid State Commun. **34**, 705 (1980).

[13]J. van Cauteren and M. Rots, in *Proceedings of the Seventeenth International Conference on Low Temperature Physics, LT-17,* edited by U. Eckern, A. Schmid, W. Weber, and H. Wühl (North-Holland, Amsterdam, 1984), p. 637.